Analyst

Cite this: *Analyst*, 2012, **137**, 4362

www.rsc.org/analyst

PAPER

Hydrogen peroxide and glucose biosensor based on silver nanowires synthesized by polyol process

Xuejuan Yang,[ab] Jing Bai,[a] Yinhu Wang,[ab] Xiue Jiang*[a] and Xiaoying He*[b]

Received 27th March 2012, Accepted 23rd June 2012
DOI: 10.1039/c2an35407a

Silver nanowires synthesized through a polyol process using polyvinylpyrrolidone as protection (PVP-AgNWs) were used as a new electrode material for constructing a sensor. Hydrogen peroxide (H_2O_2) and glucose were used as analytes to demonstrate the sensor performance of the PVP-AgNWs. It is found that the PVP-AgNWs-modified glassy carbon electrode (PVP-AgNWs/GCE) exhibits remarkable catalytic performance toward H_2O_2 reduction. This sensor has a fast amperometric response time of less than 2 s and the catalytic current is linear over the concentration of H_2O_2 ranging from 20 μM to 3.62 mM ($R = 0.998$) with a detection limit of 2.3 μM estimated on a signal-to-noise ratio of 3. A glucose biosensor was constructed by immobilizing glucose oxidase (GOD) onto the surface of the PVP-AgNWs/GCE. The resultant glucose biosensor can be used for glucose detection in human blood serum with a sensitivity of 15.86 μA mM^{-1} cm^{-2} and good selectivity and stability.

Introduction

The detection of hydrogen peroxide is of great importance in the field of food, biology, industry and medicine since it is a residual agent after disinfecting the food, a waste product of industry, a valuable marker of many oxidative biological reactions and will result in a number of diseases by reacting with a variety of targets in the cell.[1–4] Among the detection methods, electrochemical sensors have been proven to be a simple and effective way due to their high sensitivity and selectivity. Early studies focused on enzyme-based sensors.[5–8] However, the denaturation of the enzyme with certain temperature and pH affects the stability and reproducibility of the sensor,[9] and the interference of the enzyme-based sensors by other electro-oxidizable species in blood samples also limits the use of sensors *in vivo*. The good catalytic activity of silver nanoparticles towards H_2O_2 opened the door for the designing of enzymeless sensors.[10–14] In addition, H_2O_2 is also one of the oxidation products of glucose catalyzed by glucose oxidase (GOD) in the presence of O_2 where the detection of glucose can be achieved on the basis of monitoring the production of H_2O_2. Therefore, the development of enzymeless-based H_2O_2 sensors also provides a multiplex platform for the construction of glucose biosensors.[14–18] Compared with spherical nanoparticles, nanowires have promising activities in sensors due to their unique electronic properties.[19–22] In the past years, many methods have been developed to prepare high-quality silver nanowires.[23,24] Among them, polyol process-based synthesis has been recognized as one of the most popular methods and the synthesized silver nanowires can be easily transferred onto a wide range of substrates.[25] Although silver exhibits the highest electrical conductivity among all the metals,[26,27] most synthesized silver nanowires have been exploited for plasmonic applications,[23,24] and little attention has been paid to electrochemical sensing applications.[28]

In this study, we prepared silver nanowires through a polyol process using of polyvinylpyrrolidone as protection (PVP-AgNWs). The enzymeless-based H_2O_2 sensor was constructed by modification of PVP-AgNWs on a glassy carbon electrode (GCE) and the resultant sensor exhibited notable catalytic performance toward H_2O_2 reduction. Furthermore, we constructed a glucose biosensor by immobilization of GOD onto the PVP-AgNWs-modified GCE for the detection of glucose in buffer solution and human blood samples. To the best of our knowledge, this is the first time that PVP-AgNWs has been used as a new electrode material for the construction of a H_2O_2 and glucose sensor.

Experimental

Reagents and materials

NaH_2PO_4, Na_2HPO_4, NaCl, glucose, H_2O_2 (30 wt%), $AgNO_3$ and 1,2-propylene glycol (1,2-PG) were purchased from Beijing Chemical Corp. (Beijing, China). Chitosan, glucose oxidase (GOD), ascorbic acid (AA), dopamine (DA) and uric acid (UA) were obtained from Aladin Ltd. (Shanghai, China). Poly-(vinylpyrrolidone) (PVP, $M_w = 40\,000$) was obtained from Shanghai Chemical Reagent Corp. (Shanghai, China). All chemicals were used without further purification. The water used

[a]*State Key Laboratory of Electroanalytical Chemistry, Changchun Institute of Applied Chemistry, Chinese Academy of Science, Changchun 130022, China. E-mail: jiangxiue@ciac.jl.cn; Fax: +86 431-85262378; Tel: +86 431-85685653*
[b]*China west Normal University, Nanchong 637002, China. E-mail: hexysctc@yahoo.com.cn*

throughout all experiments was purified through a Millipore system. Phosphate buffer saline (PBS) was prepared by mixing stock solutions of NaH_2PO_4 and Na_2HPO_4. A fresh solution of H_2O_2 was prepared daily.

Synthesis and characterization of silver nanowires

The PVP-AgNWs were prepared by a modified polyol process.[25] In a typical preparation experiment, 10 mL 1,2-PG was mixed with PVP (150 mM as calculated in terms of the repeating unit) in a 25 mL vial. Then the mixture was heated in an oil bath at 160 °C for 1 h under stirring. After that, 1 mL NaCl solution (1 mM in 1,2-PG) was quickly added. 5 min later, 4 mL $AgNO_3$ solution (0.15 M in 1,2-PG) was added drop by drop to the stirred solution. The solution was maintained at 160 °C for another 40 min. The resultant dispersion was cooled at room temperature. The precipitate was washed with water and centrifuged at 6000 rpm for 10 min. This process was repeated for four times to purify the PVP-AgNWs. Finally, the PVP-AgNWs were re-dispersed in water and stored at 4 °C for characterization and further use.

The UV-vis absorption spectrum of the PVP-AgNWs dispersion was recorded using a Cary 500 Scan UV-visible spectrophotometer (Varian, USA) and transmission electron microscopy (TEM) measurements of the pre-prepared sample by dropping the dispersion of the PVP-AgNWs onto a carbon-coated copper grid were made on a HITACHI H-8100EM (Hitachi, Tokyo, Japan). Scanning electron microscopy (SEM) measurements were made using an XL30 ESEM FEG scanning electron microscope at an accelerating applied potential of 20 kV. Atomic force microscopy (AFM) was conducted with a SPI3800N microscope (Seiko Instruments, Inc.). The samples were prepared by dropping the dispersion onto a piece of bare glassy carbon.

Preparation of the modified electrode

The PVP-AgNWs-modified electrode was prepared by a simple casting method. Prior to coating the surface, the GCE was polished with 1.0 and 0.3 μm alumina powder, respectively, and rinsed with doubly distilled water, followed by sonication in ethanol solution and doubly distilled water successively. Then, the electrode was dried in a stream of nitrogen. After that, 15 μL of PVP-AgNWs solution (1 mg mL^{-1}) was dropped onto the surface of the pretreated GCE and left to dry at room temperature to obtain a PVP-AgNWs-modified GCE, referred to as PVP-AgNWs/GCE. The immobilization of GOD onto the surface of the PVP-AgNWs/GCE was obtained by dropping 5 μL of 30 mg mL^{-1} GOD aqueous solution onto the resultant PVP-AgNWs/GCE and kept at 4 °C for 3 h to dry, referred to as the GOD/PVP-AgNWs/GCE. Prior to amperometric experiment, 2 μL of chitosan (0.2%) was additionally dropped onto the surface of the resultant-modified electrode and dried at 4 °C for 2 h.

Electrochemical measurements

Amperometric and cyclic voltammetric (CV) experiments were carried out by using a computer-controlled CHI830D electrochemical analyzer (CH Instruments, Inc., Shanghai) in a home-made three-electrode electrochemical cell consisting of a GCE (geometric area = 0.07 cm^2) as the working electrode, a twisted platinum wire as an auxiliary electrode, and an Ag/AgCl (in saturated KCl) as the reference electrode. In steady-state amperometric experiments, the potential was set as −0.3 V and the PBS was stirred with a magnetic stirrer bar at a stirring rate of 300 rpm. The current–time curve was recorded after a constant background current had been established. The PBS was purged with high-purity nitrogen for at least 30 min prior to experiments and a nitrogen atmosphere was kept over the solution in the cell. All electrochemical experiments were performed at the room temperature. All experiments were performed in compliance with the relevant laws and institutional guidelines, and also approved by the institutional committees.

Results and discussion

Characterization of the prepared PVP-AgNWs

Fig. 1a shows the UV-vis absorption spectrum of the PVP-AgNWs dispersed in water. The appearance of an apparent plasmon peak at 379 nm corresponds to the transversal plasmon mode and a shoulder peak at 427 nm indicates the formation of the PVP-AgNWs with a diameter larger than 40 nm.[29] The morphology of the PVP-AgNWs was observed by the TEM image as shown in Fig. 1b. It can be seen from the main low-magnification TEM image that the resultant nanowires are continuous and uniform in diameter with an average length of 5–6 μm. From the enlarged image (Fig. 1b, inset), we can conclude that the most important feature of these nanowires is their rectangular cross-sections with an average diameter of ~80 nm. The aspect ratio (l/d) of the PVP-AgNWs is 69 ± 9.

Electrocatalytic behavior of the PVP-AgNWs toward H_2O_2 reduction

To demonstrate the sensing application of the PVP-AgNWs, we first constructed an enzymeless-based H_2O_2 sensor by modification of the PVP-AgNWs on the surface of a GCE.

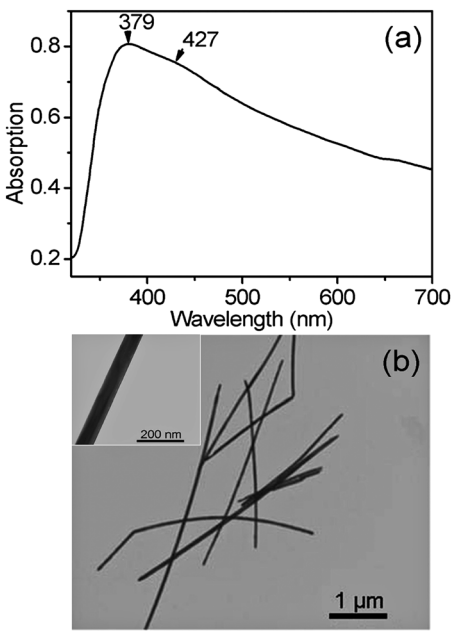

Fig. 1 (a) UV-vis spectra of AgNWs dispersed in aqueous solution. (b) Low and high (inset) magnification TEM images of the PVP-AgNWs.

At the same time, we characterized the surface morphology of the PVP-AgNWs dropped onto a GCE. Fig. 2 shows representative the SEM image of the film formed on the GC substrate. It can be seen that as-formed PVP-AgNWs can form a multilayered film on the GC substrate with a random coverage. When addition of 1 mM H_2O_2 to N_2-saturated PBS (0.2 M, pH 6.5), the PVP-AgNWs/GCE exhibits a remarkable catalytic reduction peak at −0.62 V (*vs.* Ag/AgCl) with the intensity of about 23 μA (Fig. 3a, dash-dotted line) in comparison with its CV response without H_2O_2 (solid line). To verify that the catalytic current was from PVP-AgNWs, two control experiments were performed on a bare GCE (dashed line) and a PVP/GCE (dotted line), respectively. It is clearly seen that the responses of both the bare GCE and PVP/GCE toward the reduction of H_2O_2 are quite weak in the potential range between −0.2 and 0.8 V. It is also seen that the peak current of the reduction of H_2O_2 increases with increasing the concentration of H_2O_2 from 1 to 8 mM (Fig. 3b). All these observations show that the PVP-AgNWs exhibit a notable catalytic performance for H_2O_2 reduction. In addition, the relative standard deviation (RSD) of the amperometric response to 1 mM H_2O_2 was 3.9% for 5 successive measurements, indicating the good reproducibility of the PVP-AgNWs toward the catalysis of H_2O_2. The stability of the sensor was tested by measuring the response current of the PVP-AgNWs/GCE to 1 mM H_2O_2 in N_2-saturated PBS (0.2 M, pH 6.5). After 7 days, the reduction current of H_2O_2 was only reduced by 8.4%, indicating the good stability of PVP-AgNWs-based sensor for H_2O_2 detection.

Fig. 4 shows a typical current–time plot of the PVP-AgNWs/GCE upon successive additions of H_2O_2 into stirring PBS at an applied potential of −0.3 V. Owing to the low operating potential, those co-existing electroactive substances had no interference on the H_2O_2 reduction.[30] The response current dramatically increased after each addition of H_2O_2 and could achieve 95% of the steady-state current in less than 2 s. The inset of Fig. 4 is the corresponding calibration plot. The linear detection range is estimated to be 0.02–3.62 mM ($R = 0.998$) and the detection limit is estimated to be 2.30 μM, at a signal-to-noise ratio of 3.

Although the PVP-AgNWs/GCE shows equivalent electrocatalytic properties toward H_2O_2 reduction as the Ag nanoparticles-modified GCE in response time, linear range, reproducibility and stability,[12,14,31] the detection limit of 2.30 μM of the PVP-AgNWs/GCE is notably lower than those at the Ag nanoparticles-based modified GCE: for instance, the Ag nanoparticles–graphene-modified electrode (7 μM),[32] the Ag@PMPD–Ag core–shell nanoparticles-modified electrode (2.5 μM),[33] the AgNP/rGO nanocomposites-modified electrode (7.1 μM),[34] AgNP/rGO hybrids-modified electrode (31.3 μM),[35] AgNP-decorated poly(*m*-phenylenediamine) (PMPD) microparticles (4.7 μM),[36] AgNP-PQII/graphene (28 μM),[37] AgNPs-NFs/GCE (62 μM),[12] AgNPs/F-SiO_2/GO (4 μM),[14] PQII-AgNPs (33.9 μM)[31] and PEDOT/AgNPs (7 μM).[8] The random coverage of the AgNWs on the GCE as shown in Fig. 2 might affect the performance of the sensor.

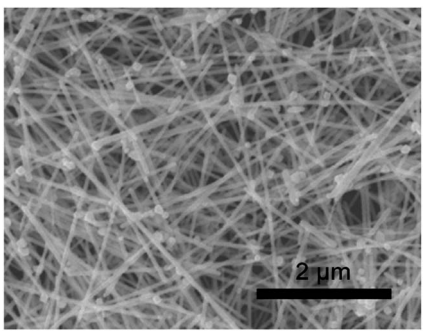

Fig. 2 SEM image of the PVP-AgNWs on the bare GCE.

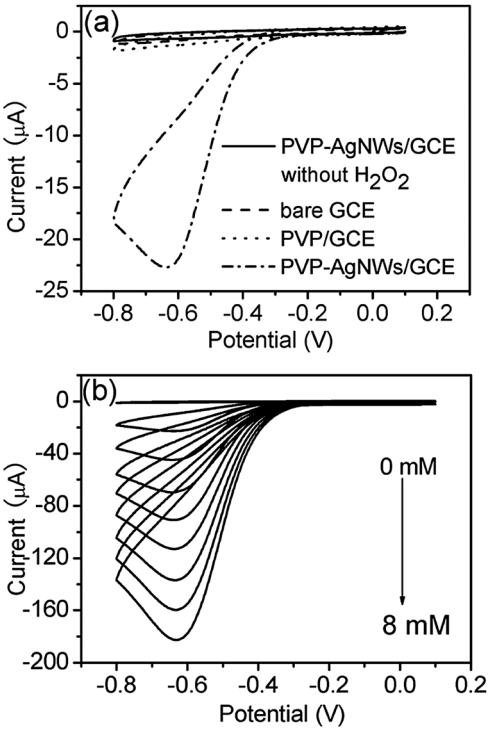

Fig. 3 (a) CVs of different electrodes in N_2-saturated 0.2 M PBS at pH 6.5 in the presence of 1 mM H_2O_2 at a scan rate of 50 mV s^{-1}. (b) CVs of the PVP-AgNWs/GCE in N_2-saturated 0.2 M PBS at pH 6.5 upon increase of H_2O_2 concentrations from 1 to 8 mM with an increased step size of 1 mM (scan rate: 50 mV s^{-1}).

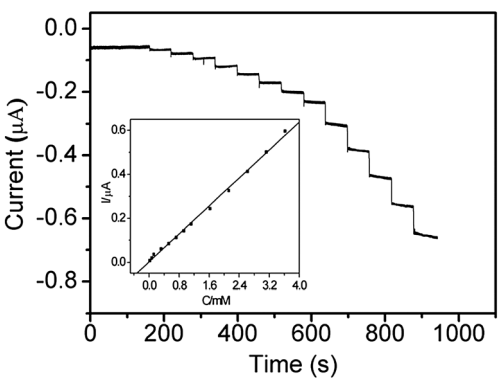

Fig. 4 Typical time–current response of the PVP-AgNWs/GCE to the successive injection of H_2O_2 into the stirred N_2-saturated 0.2 M PBS at pH 6.5 at the applied potential of −0.3 V. Inset shows the corresponding calibration plot for H_2O_2.

Direct electrochemistry of adsorbed glucose oxidase at the PVP-AgNWs/GCE

Due to its good electrocatalytic activity of the PVP-AgNWs to H_2O_2, a GOD-based biosensor was further developed by immobilizing GOD onto the surface of the PVP-AgNWs-modified GCE. The surface morphology of the GOD/PVP-AgNWs composite membrane on the GCE was examined by SEM as shown in Fig. 5. Compared with the PVP-AgNWs surface image (Fig. 2), the morphology of the PVP-AgNWs is obviously unclear due to the decrease of the conductivity of the PVP-AgNWs by the protein coating. The AFM image clearly indicates that the adsorption of GOD on a single PVP-AgNW is relatively homogenous (inset). Fig. 6a shows the CVs of the bare GCE (dotted line), PVP-AgNWs/GCE (dashed line), and GOD/PVP-AgNWs/GCE (solid line) in N_2-saturated 0.2 M PBS (pH 7.4) at a scan rate of 0.4 V s^{-1}. Obviously, the bare GCE and PVP-AgNWs/GCE did not lead to redox peaks. However, a pair of well-defined redox peaks at −0.43 V and −0.47 V was observed for the GOD/PVP-AgNWs/GCE, which should result from direct electron transfer of the immobilized GOD upon the conversion of GOD (FAD) to GOD ($FADH_2$).[38] The peak potential separation is about 40 mV. The well-defined and quasi-reversible redox peaks suggest favorable direct electron transfer between the electrode and redox centers of the GOD molecules. The formal potential ($E^{\circ\prime}$) calculated by averaging the cathodic and anodic peak potentials is estimated as −0.48 V. This value is close to the standard electrode potential of −0.51 V (*vs.* Ag/AgCl) for FAD/$FADH_2$ at pH 7.0 (25.8 °C),[39] suggesting that the GOD molecules retain their bioactivity after adsorption on the PVP-AgNWs.

The influence of varying the scan rate on the cyclic voltammetric performance of the immobilized GOD is shown in Fig. 6b. The anodic and cathodic peak currents increase linearly with an increase of the scan rate from 0.05 to 0.6 V s^{-1} (the inset of Fig. 6b), indicating that the redox process of the immobilized GOD is a surface-controlled process.

Electrochemical detection of glucose at the GOD/PVP-AgNWs/GCE

Fig. 7 shows the CVs of the GOD/PVP-AgNWs/GCE in 0.2 M PBS at pH 7.4 solution containing different concentrations of glucose under the condition of oxygen (O_2) saturation. A strong reduction peak at about −0.63 V should correspond to the reduction of O_2 and H_2O_2. The reduction current increases gradually with the successive addition of glucose into the O_2-saturated PBS solution. Since GOD can selectively catalyze the oxidation of glucose to gluconic acid and H_2O_2 in the presence of oxygen, the accumulation of the H_2O_2 produced by the oxidation of increased glucose results in a continuous enhancement of the

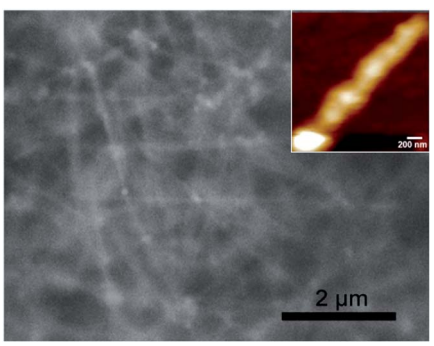

Fig. 5 SEM and AFM (inset) images of adsorbed GOD on the PVP-AgNWs/GCE.

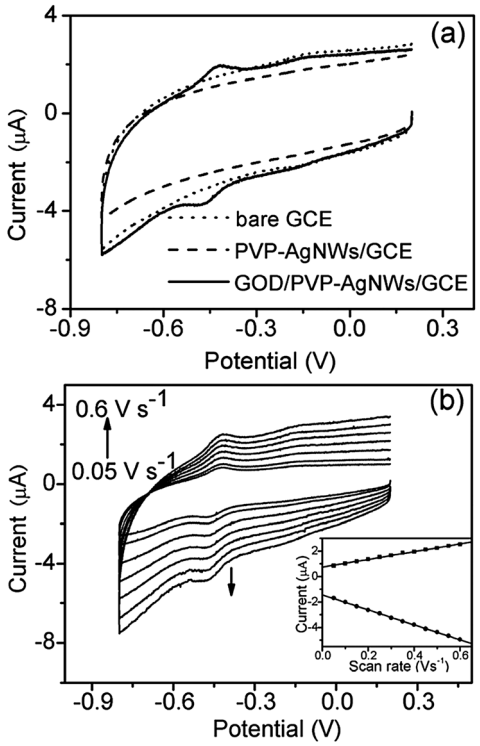

Fig. 6 (a) CVs of bare GCE, PVP-AgNWs/GCE and GOD/PVP-AgNWs/GCE in 0.2 M PBS solution (pH 7.4) saturated with N_2 at a scan rate of 0.4 V s^{-1}. (b) CVs of the GOD/PVP-AgNWs/GCE in N_2-saturated PBS solution (pH 7.4) at different scan rates (from inside to outside): 0.05, 0.1, 0.2, 0.3, 0.4, 0.5 and 0.6 V s^{-1}. The inset shows the linear dependence of anodic and cathodic peak currents *vs.* scan rate in the range of 0.05–0.6 V s^{-1} with the interval of 0.05 V s^{-1}.

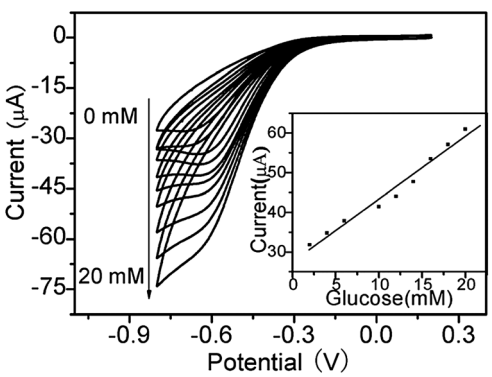

Fig. 7 CVs of the GOD/PVP-AgNWs/GCE in PBS solution (pH 7.4) in the presence of different glucose concentrations under O_2 saturation, from top to bottom: 0, 2, 4, 6, 10, 12, 14, 16, 18, 20 mM. Inset is the calibration curve corresponding to amperometric responses at the reduction peak ($R = 0.987$).

reductive current of H_2O_2. The inset of Fig. 7 shows the linear relationship between the catalytic current and glucose concentration range from 2 to 20 mM ($R = 0.987$). The sensitivity of the glucose detection is 22.43 μA mM^{-1} cm^{-2} and the relative standard deviation (RSD) of the current response to 5 mM glucose is 4.4% for 6 successive measurements, indicating a good repeatability of the biosensor. Compared to the RSD of the Pt NPs-based glucose biosensor, 5.2%,[40] the biosensor designed here has better reproducibility.

Stability and selectivity of the GOD/PVP-AgNWs/GCE

The long-term stability of the biosensor was tested by periodical measurements of the responses of the biosensor to 3 mM glucose in PBS solution (pH 7.4) at a scan rate of 50 mV s^{-1}. The biosensor was kept at 4 °C when not used. As shown in Fig. 8a, on the 2nd day, 96% of the initial response current can be obtained. On the 5th day, about 81% of the initial response current can be obtained. The loss of the response current may be ascribed to the decrease of the enzyme activity during these days.[41] The negligible decrease of the response current over the investigation period implies that the electrode can be used over a long period.

To evaluate the selectivity of the biosensor, the current responses of the biosensor to several possible interfering substances, such as ascorbic acid (AA), uric acid (UA), and dopamine (DA), which normally co-exist with glucose in human blood, were examined, as shown in Fig. 8b. The current response of the biosensor to 5 mM glucose was not affected by the co-existence of 0.5 mM of AA, UA and DA in 0.2 M PBS (pH 7.4), indicating the anti-interference of the biosensor to the detection of glucose in real blood samples. It can be concluded that the GOD/PVP-AgNWs electrode shows high selectivity for glucose detection. The sensitivity, linearity and anti-interference of the designed biosensor prove to be possible for glucose measurement in real sample analysis.

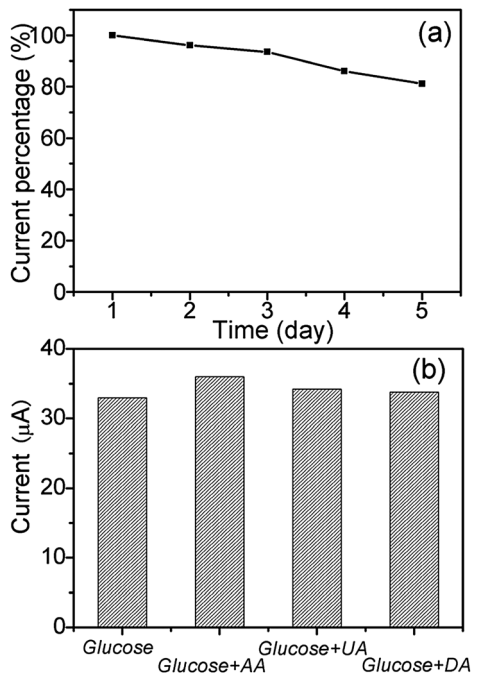

Fig. 8 (a) The response current of 3 mM glucose at the GOD/PVP-AgNWs/GCE in PBS solution (pH 7.4) at a scan rate of 50 mV s^{-1} was plotted as a function of time. (b) Comparison of the responses of the GOD/AgNWs/GCE to 5 mM glucose, 5 mM glucose mixed with 0.5 mM ascorbic acid (AA), uric acid (UA), and dopamine (DA) in O_2-saturated 0.2 M PBS (pH 7.4).

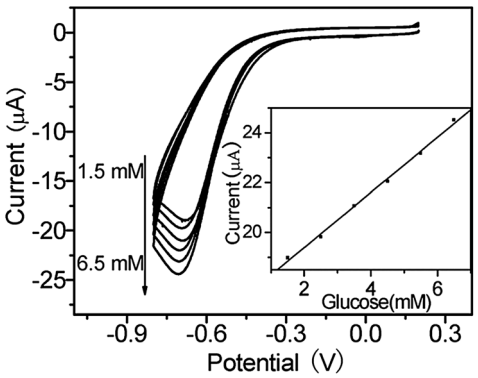

Fig. 9 CVs of the GOD/PVP-AgNWs/GCE in a real blood serum sample mixed with pH 7.4 PBS solution in the presence of glucose concentrations varied from 1.5 to 6.5 mM with an increased step of 1 mM under O_2 saturation. Inset is the calibration curve corresponding to amperometric responses at the reduction peak ($R = 0.998$).

Real sample analysis

It is well known that the blood glucose level of a normal person ranges from 4 to 6 mM.[42] Therefore, the linear range of the designed biosensor here is suitable for its practical application for the determination of human blood sugar concentrations. To illustrate the feasibility of the biosensor in practical analysis, the GOD/AgNWs/GCE was used to detect glucose in human blood (from a local hospital). The original glucose concentration of the human blood sample is hypothesized as 5 mM. The test was carried out by mixing 3.5 mL phosphate buffer with 1.5 mL physiological blood. Fig. 9 shows that the cathodic current increases with successive addition of 1 mM glucose into the blood sample saturated with O_2, and the inset of Fig. 9 shows the linear relationship between the catalytic current and the increased glucose concentration from 1.5 to 6.5 mM ($R = 0.998$) with the sensitivity of 15.86 μA mM^{-1} cm^{-2}, which is better than the AuNPs–graphene composite biosensor.[16]

Conclusions

In summary, we have successfully constructed a H_2O_2 and glucose sensor by dropping of PVP-AgNWs onto the surface of a GCE. The resultant electrode showed high electrocatalytic activity toward H_2O_2 without using an enzyme. Furthermore, a glucose oxidase was adsorbed onto the nanowire surface to fabricate a glucose biosensor. The resulting biosensor exhibited good amperometric response to glucose in PBS and human blood serum. It also presented a number of other attractive features such as fast response, long-term storage stability, high reproducibility and satisfactory anti-interference ability. The silver nanowires-based sensor developed here offers a new approach

for constructing novel biosensors and meanwhile extends the application of silver nanowires.

Acknowledgements

This work was financially supported by the Youth Foundation of Jilin Province (201101081), President Funds of the Chinese Academy of Sciences.

References

1 A. Schwake, B. Ross and K. Cammann, *Sens. Actuators, B*, 1998, **46**, 242.
2 Y. Wang, J. Huang, C. Zhang, J. Wei and X. Zhou, *Electroanalysis*, 1998, **10**, 776.
3 J.-W. Lee and J. D. Helmann, *Nature*, 2006, **440**, 363.
4 M. A. Yorek, *Free Radical Res.*, 2003, **37**, 471.
5 J. Jia, B. Wang, A. Wu, G. Cheng, Z. Li and S. Dong, *Anal. Chem.*, 2002, **74**, 2217.
6 X. Jiang, L. Zhang and S. Dong, *Electrochem. Commun.*, 2006, **8**, 1137.
7 C.-Y. Liu and J.-M. Hu, *Biosens. Bioelectron.*, 2009, **24**, 2149.
8 A. Balamurugan and S.-M. Chen, *Electroanalysis*, 2009, **21**, 1419.
9 Y. Shimizu and K. Morita, *Anal. Chem.*, 1990, **62**, 1498.
10 M. R. Guascito, E. Filippo, C. Malitesta, D. Manno, A. Serra and A. Turco, *Biosens. Bioelectron.*, 2008, **24**, 1057.
11 Y. Song, K. Cui, L. Wang and S. Chen, *Nanotechnology*, 2009, **20**, 105501.
12 J. Tian, S. Liu and X. Sun, *Langmuir*, 2010, **26**, 15112.
13 S. Liu, J. Tian, L. Wang and X. Sun, *J. Nanopart. Res.*, 2011, **13**, 4539.
14 W. Lu, Y. Luo, G. Chang and X. Sun, *Biosens. Bioelectron.*, 2011, **26**, 4791.
15 Y. Song, K. Qu, C. Zhao, J. Ren and X. Qu, *Adv. Mater.*, 2010, **22**, 2206.
16 C. Shan, H. Yang, D. Han, Q. Zhang, A. Ivaska and L. Niu, *Biosens. Bioelectron.*, 2010, **25**, 1070.
17 G. Chang, Y. Luo, W. Lu, X. Qin, A. M. Asiri, A. O. Al-Youbi and X. Sun, *Catal. Sci. Technol.*, 2012, **2**, 800.
18 X. Qin, W. Lu, Y. Luo, G. Chang, A. M. Asiri, A. O. Al-Youbi and X. Sun, *Analyst*, 2012, **137**, 939.
19 S. Hui, J. Zhang, X. Chen, H. Xu, D. Ma, Y. Liu and B. Tao, *Sens. Actuators, B*, 2011, **155**, 592.
20 X. Ren, F. Tang, R. Liao and L. Zhang, *Electrochim. Acta*, 2009, **54**, 7248.
21 Y. Lu, M. Yang, F. Qu, G. Shen and R. Yu, *Bioelectrochemistry*, 2007, **71**, 211.
22 U. Yogeswaran and S. Chen, *Sensors*, 2008, **8**, 290.
23 M. Rycenga, C. M. Cobley, J. Zeng, W. Li, C. H. Moran, Q. Zhang, D. Qin and Y. Xia, *Chem. Rev.*, 2011, **111**, 3669.
24 X. Li, L. Wang and G. Yan, *Cryst. Res. Technol.*, 2011, **46**, 427.
25 Y. Bi, H. Hu and G. Lu, *Chem. Commun.*, 2010, **46**, 598.
26 A. Rad, A. Mirabi, E. Binaian and H. Taybi, *Int. J. Electrochem. Sci.*, 2011, **6**, 3671.
27 Y. Sun, *Science*, 2002, **298**, 2176.
28 M.-J. Song, S. W. Hwang and D. Whang, *J. Appl. Electrochem.*, 2010, **40**, 2099.
29 Y. Xiong, Y. Xie, C. Wu, J. Yang, Z. Li and F. Xu, *Adv. Mater.*, 2003, **15**, 405.
30 B. Wolfrum, M. Zevenbergen and S. Lemay, *Anal. Chem.*, 2008, **80**, 972.
31 W. Lu, F. Liao, Y. Luo, G. Chang and X. Sun, *Electrochim. Acta*, 2011, **56**, 2295.
32 Y. Zhang, S. Liu, L. Wang, X. Qin, J. Tian, W. Lu, G. Chang and X. Sun, *RSC Adv.*, 2012, **2**, 538.
33 J. Tian, Y. Luo, H. Li, W. Lu, G. Chang, X. Qin and X. Sun, *Catal. Sci. Technol.*, 2011, **1**, 1393.
34 S. Liu, L. Wang, J. Tian, Y. Luo, X. Zhang and X. Sun, *J. Colloid Interface Sci.*, 2011, **363**, 615.
35 S. Liu, J. Tian, L. Wang and X. Sun, *Carbon*, 2011, **49**, 3158.
36 J. Tian, H. Li, W. Lu, Y. Luo, L. Wang and X. Sun, *Analyst*, 2011, **136**, 1806.
37 S. Liu, J. Tian, L. Wang, H. Li, Y. Zhang and X. Sun, *Macromolecules*, 2010, **43**, 10078.
38 C. Fu, W. Yang, X. Chen and D. G. Evans, *Electrochem. Commun.*, 2009, **11**, 997.
39 Z. H. Dai, J. Ni, X. H. Huang, G. F. Lu and J. C. Bao, *Bioelectrochemistry*, 2007, **70**, 250.
40 X. Kang, Z. Mai, X. Zou, P. Cai and J. Mo, *Talanta*, 2008, **74**, 879.
41 Y. Zhang, G. Chang, S. Liu, W. Lu, J. Tian and X. Sun, *Biosens. Bioelectron.*, 2011, **28**, 344.
42 C. Shan, H. Yang, J. Song, D. Han, A. Ivaska and L. Niu, *Anal. Chem.*, 2009, **81**, 2378.